

# WIDE ANGLE RADAR IMAGING UNDER LOW SNR VIA SPARSITY ENHANCED NON-NEGATIVE MATRIX FACTORIZATION

Ran Xu, Yachao Li and Mengdao Xing, Member, IEEE

National Laboratory of Radar Signal Processing, Xidian University, Xi'an, China

## ABSTRACT

Narrow angle approximation and isotropic assumption adopted in regular radar imaging are violated in wide angle radar imaging scenario. Therefore, conventional Fourier based methods are not directly applicable, and full aperture algorithms perform poor under low SNR. This paper proposes an imaging scheme based on Sparsity Enhanced Non-negative Matrix Factorization (SENMF). The full aperture is firstly divided into several overlapping subapertures, to which Polar Format Algorithm (PFA) is then applied to obtain subimages at different aspects. Finally, NMF with sparsity regularization is exploited to iteratively composite the full aperture image, which demonstrates enhanced target feature and improved SNR. The results of Backhoe data processing verify the validity of the novel approach.

*Index Terms*— SAR, SENMF, PFA

## 1. INTRODUCTION

Wide angle radar imaging (WARI) acquires higher azimuth resolution by transmitting and receiving echoes through a larger angular extent [1]-[3]. A series of challenges arise in this situation. The support region of the wavenumber spectrum of the data turns into a sector with large angular occupation, so the rectangular grid approximation can be no longer valid. Long synthesized aperture leads to severe scatterer migration through range cells (MTRC) and time-varying Doppler histories. Additionally, anisotropic scattering mechanism is more appropriate rather than isotropic mechanism. Therefore, narrow angle assumption used in conventional SAR is not a reasonable choice for wide angle imaging, and Fourier based imaging algorithms cannot be utilized directly.

Aiming at these problems, the common solution is to divide the whole imaging interval into several overlapping (or non-overlapping) subapertures. Reference [4] employs linear image approximation for subintervals, thus 2-D FFT can be performed on each sub data block followed by image rotation and composition processing. Since no scatterer migration is allowed, the algorithm is application-limited. In [1] and [5], the authors convert the wide angle imaging to an

inverse problem; subimages are obtained via solving a complex optimization, and full aperture image composition is then applied. The final image benefits from super resolution potential of the method, which however relies on the exhaustive creation of SAR projection operator. Besides, iterative optimization of each subimage can be a computational challenge.

Non-negative Matrix Factorization, as a robust tool for feature analysis and extraction, is widely used in areas such as signal processing and pattern recognition [6]-[7]. There have been several publications that focus on NMF applications related to remote sensing issues [8]-[10], but no radar imaging algorithms are involved. We propose a novel scheme for wide angle radar imaging based on Sparsity Enhanced NMF (SENMF). Subaperture technique and Polar Format Algorithm (PFA) are employed to acquire subimages, and we rebuild the full aperture image via NMF with sparseness regularization term. The final image shows its superiority in feature enhancement and noise suppression. The modified multiplicative update rule we derive guarantees the non-negativity of results.

## 2. SIGNAL MODEL

Larger integration interval means higher azimuth resolution, more scattering information, and higher recognition probability. For example, Spotlight mode SAR is a wise choice to increase the illumination time for the purpose of capturing clear features of a ground target. The target is assumed to be consisted of several anisotropic scatterers. Let the radar transmits linear frequency modulated (LFM) pulses, then the wide angle baseband signal of the target scene after pre-processing procedures of demodulation, match-filtering and motion compensation[11] can be modeled by:

$$s f, \theta = \iint_V \sigma(x, y; \theta) \exp -jK_x x - jK_y y \, dx dy \quad (1)$$

where  $\sigma(x, y; \theta)$  is the angle-dependent spatial reflectivity function at location  $(x, y)$ ,  $V$  is the illuminated area,  $K_x = 4\pi f \sin \theta / c$ ,  $K_y = 4\pi f \cos \theta / c$  respectively denote the range wavenumber and azimuth wavenumber,  $\theta \in [-\Theta/2, \Theta/2]$  is the azimuth observation angle where  $\Theta$  is the total integration angle range,

$f \in [f_c - B/2, f_c + B/2]$  represents the signal frequency,  $f_c$  is carrier frequency and  $B$  is bandwidth.

In WARI mode, the support region of the spectrum almost resembles an incomplete annular ring which possesses a large angular range. Consequently, there exist limits to effective interpolation region. Direct PFA implementation should meet the upper bound requirement of  $\Theta$  [3], and utilization ratio of the spectrum might be low. Such restrictions do not apply to full aperture algorithms, which however may provide limited information as explained in Section I.

The subaperture technique is a robust alternative. By sequentially partitioning full aperture data into sub-blocks, the performance of PFA can be guaranteed and the anisotropic effect is alleviated within each subaperture. SNR can also be increased via subimage fusion. The subaperture data can be addressed as follows:

$$s^n(f, \theta) = s(f, \theta) \text{rect} \left[ \frac{\theta + (\Theta - \Omega) / 2 - (n-1)\Delta\theta}{\Omega} \right] \quad (2)$$

For where  $s^n(f, \theta)$  denotes the  $n$ th of total  $N$  sub-blocks,  $\Omega$  denotes the total integration angle of subaperture,  $\Delta\theta$  is the aspect increment between subapertures. We set  $\Delta\theta$  to be smaller than  $\Omega$  to allow an angular overlapping of length  $\Omega - \Delta\theta$ . Since PFA makes no full use of the spectrum, overlapping could avoid gaps among sub-blocks. By this way we can also smooth the variation of scattering reflectivity over subimages. Moreover, the phase histories of reflectors with narrow azimuth response persistence can be prevented from being split up in case the amplitude is weakened in the image.

PFA can now be applied to subapertures, each corresponding subimage demonstrates features at a certain aspect. To obtain the full aperture image, the subimages should be composited after rotational alignment (rotate  $n$ th subimage around the scene reference point by  $(n-1)\Delta\theta$ ). Full aperture image composition is essentially a process of image fusion. We present a scheme based on SENMF, by which wide angle radar image with more explicit features and improved SNR is acquired, thus the recognizability and interpretability of a target are enhanced.

### 3. IMAGE FORMATION VIA SENMF

Non-negative Matrix Factorization can be described as: given a non-negative matrix  $\mathbf{V} \in \mathbb{R}^{m \times n}$ , find non-negative matrices  $\mathbf{W} \in \mathbb{R}^{m \times r}$  and  $\mathbf{H} \in \mathbb{R}^{r \times n}$  that satisfy:

$$\mathbf{V} \approx \mathbf{W}\mathbf{H} \quad (3)$$

where  $r$  meets  $(m+n)r < mn$ . NMF can be deemed as a process that projects original data  $\mathbf{V}$  into a lower dimensional feature subspace to obtain an approximate linear representation with self-learned basis set. According to the principle of NMF, when  $r=1$ , each data sample vector of  $\mathbf{V}$  can be rebuilt via the only basis which therefore should

integrate the entire feature information of the input data samples. If we let the subimages be the input samples to facilitate NMF, the unique output image vector  $\mathbf{W}$  should contain all scattering characteristics at each azimuth observations. Furthermore, imposing sparse constraint on NMF algorithm can reinforce the sparsity in factorization results, which is beneficial to resolution enhancement, noise (clutter) reduction and side lobe suppression.

#### 3.1 Derivation of SENMF

We now derive the general case for our method SENMF, i.e.  $r \neq 1$ , and the sparseness of each basis in  $\mathbf{W}$  can be individually controlled. Compared with  $l_2$ -norm and  $l_1$ -norm, imposing  $l_k$ -norm ( $0 < k < 1$ ) constraint on optimization leads to a sparser structure in solution [11]. We consider Euclid distance as the cost function of NMF and apply  $l_k$ -norm ( $0 < k < 1$ ) penalty term to basis matrix, resulting in the following optimization problem:

$$\min_{\mathbf{W} \in \mathbb{R}^{m \times r}, \mathbf{H} \in \mathbb{R}^{r \times n}} F(\mathbf{W}, \mathbf{H}) = \min \left\{ \frac{1}{2} \|\mathbf{V} - \mathbf{W}\mathbf{H}\|_F^2 + \sum_{a=1}^r \alpha_a \|\mathbf{W}(:, a)\|_{k_a}^{k_a} \right\} \quad (4)$$

s.t.  $W_{ia} \geq 0, H_{aj} \geq 0$

where  $\mathbf{W}(:, a)$  is the  $a$ th column vector of  $\mathbf{W}$ ,  $[\cdot]_{ia}$  represents the  $i$ th row  $a$ th column element of a matrix.

Gradient descent based algorithms are commonly used in solving NMF. Iterations proceed as follows:

$$\begin{aligned} W_{ia}^{(p)} &= W_{ia}^{(p-1)} - \mu_{ia} \left( \partial F(\mathbf{W}, \mathbf{H}) / \partial W_{ia} \right) \\ H_{aj}^{(p)} &= H_{aj}^{(p-1)} - \delta_{aj} \left( \partial F(\mathbf{W}, \mathbf{H}) / \partial H_{aj} \right) \end{aligned} \quad (5)$$

where  $p$  is the count of iterations,  $\mu_{ia}, \delta_{aj}$  denote the step size parameters.

Motivated by Lee and Seung's multiplicative update rule [12] which is both non-negativity and convergence guaranteed, we design the step sizes in terms of our cost function and arrive at the modified multiplicative update rule:

$$\begin{aligned} W_{ia}^{(p)} &= W_{ia}^{(p-1)} \frac{(\mathbf{V}\mathbf{H}^T)_{ia}}{(\mathbf{W}^{(p-1)}\mathbf{H}\mathbf{H}^T)_{ia} + \alpha_a k_a (W_{ia}^{(p-1)})^{k_a-1} + \varepsilon} \\ H_{aj}^{(p)} &= H_{aj}^{(p-1)} \frac{(\mathbf{W}^T\mathbf{V})_{aj}}{(\mathbf{W}^T\mathbf{W}\mathbf{H}^{(p-1)})_{aj} + \varepsilon} \end{aligned} \quad (6)$$

The merits of the algorithm lie in the preservation of non-negativity and the elimination of step size parameters needed in additive gradient descent model.

#### 3.2 Full Aperture Image Composition with SENMF

As is explained in the beginning of this section, if we let subimages be the input vectors of  $\mathbf{V}$  and set  $r=1$ , then the unique output basis should contain target information of each subimage. Particularly, we exploit SENMF to produce

extra sparseness boost, which has the potential of feature enhancement and noise reduction. The full aperture image formation with SENMF consists of following steps:

- 1). Perform PFA on each subaperture data block  $s^n(f, \theta)$  to obtain subimages.
- 2). Rotate the  $n$ -th subimage by  $(n-1)\Delta\theta$ , and denote the resulted magnitude matrix as  $\mathbf{I}_n$ .
- 3). Vectorize  $\mathbf{I}_n$  by stacking the columns to form a vector of length  $M$  and normalizing it for initialization is also mandatory.
- 4). Let subimage vectors be the input of SENMF
- 5). Iterate according to (6), the output  $\mathbf{w}_{opt}$  is the feature basis extracted from all the subimages.
- 6). Apply inverse transform  $\text{vec}(\cdot)^{-1}$  to  $\mathbf{w}_{opt}$ , then the composite full aperture image with enhanced SNR is obtained.

It should be emphasized that subaperture technique and PFA will both cause azimuth resolution to decrease. However, the composite image is not significantly worse than images obtained via full aperture processing such as BP. Because scattering response persistence is limited [14] and self-occlusion may happen in WARI, so there always exists an underlying upper-bound of azimuth resolution of a scatterer. Furthermore, SENMF can improve the point resolvability by introducing sparsity constraint.

### 3. SIMULATION EXPERIMENTS

We utilize the Backhoe public data [15] with  $110^\circ$  observation extent and 7GHz-13GHz frequency range to verify our approach. The original data is deliberately contaminated by -5dB additive Gaussian noise. The effective interpolation region of the data is too small for full aperture PFA. Fig.1 gives the reconstructed image by full aperture BP algorithm. It can be seen that the target is not well described especially the weak components. Fig.2(a)-(c) give the reconstructed full aperture images via direct image summation, GLRT and SENMF ( $\alpha = 0.6, k = 0.8$ ) respectively.

Tab.1 Comparison of different imaging results

	BP	Summation	GLRT	NMFSC	SENM F
Entropy	11.433 8	10.9040	10.714 9	6.9898	6.8499
Sparseness	0.2916	0.1797	0.2113	0.9038	0.9038
TBR(dB)	14.217 2	28.1161	13.621 3	61.0913	85.1731

Results show that these subaperture algorithms outperform BP in feature preservation and noise reduction despite a relatively lower resolution. Weak scatterers are better visualized; therefore more information can be extracted for recognition purposes. It is also obvious that our method is superior in suppressing noise and enhancing weak details without disturbing the energy distribution.

We set the sparseness degree of SENMF result ( $\text{sp} = 0.9038$ ) as the desired value to feed the NMFSC algorithm [13], which performed poorer in sparsity improvement and target description than SENMF as Fig. 2(d) illustrates. Comparisons of entropy, sparseness and Target-to-Background Ratio (TBR) of the final images are also given in Tab.1. The wide angle image via our approach shows the smallest entropy and the highest TBR, which mean the best interpretability of the target.

### 4. CONCLUSIONS

This paper presents a novel way to iteratively reconstruct wide angle radar images with subaperture technique. Subimages are first obtained using PFA, and then the full aperture image composition is achieved by exploiting NMF with sparsity enhancing auxiliary function. Modified multiplicative update rule is derived in detail to mathematically solve the SENMF problem. Imaging results of low SNR Backhoe data prove the promising capability of SENMF in radar image enhancement and noise reduction. Additionally, SENMF are also potentially applicable to other applications such as multi-static imaging [16] and ISAR image fusion [17, 18], where our future research will head toward.

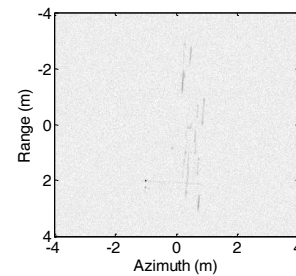


Fig.1. Image reconstructed via BP

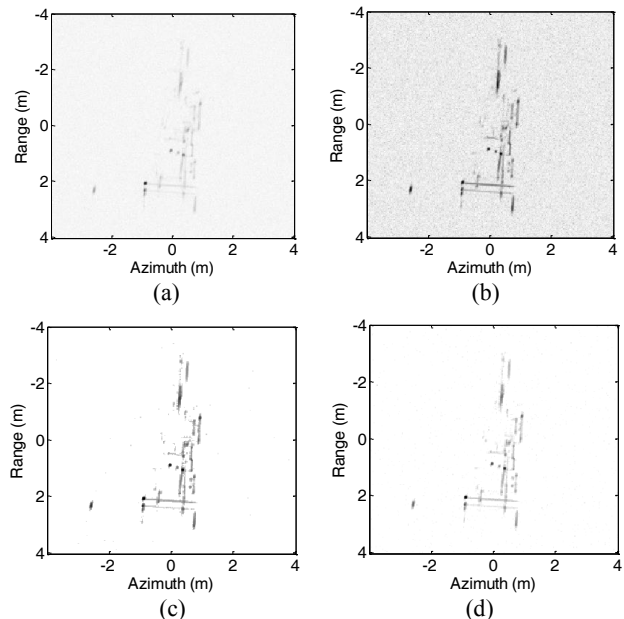


Fig.2. Images reconstructed via subaperture technique using (a) direct image summation (b) GLRT (c) our method (d) NMFSC (29 overlapping subapertures,  $\Theta = 28^\circ, \Delta\theta = 2.9^\circ$ )

[18] Z. Li, S. Papson, and R. M. Narayanan, "Data-level fusion of multilook inverse synthetic aperture radar images," *IEEE Trans. Geosci. Remote Sens.*, vol. 46, no. 5, pp. 1394 – 1406, May 2008.

## 5. REFERENCES

- [1] R. L. Moses, L. C. Potter, and M. Cetin, "Wide angle SAR imaging," in *SPIE Proc. Defense and Security Symposium*, Orlando, 2004, pp.164-175.
- [2] D. A. Ausherman, A. Kozma, J. L. Walker, H. M. Jones, and E. C. Poggio, "Developments in radar imaging," *IEEE Trans. Aerosp. Electron. Syst.*, vol. 20, no. 4, pp. 363–400, Jul. 1984.
- [3] F. Zhou, X. Bai, M. Xing, and Z. Bao, "Analysis for wide-angle radar imaging," *IET Radar, Sonar and Nav.*, vol.5, no.4, pp.449-457, Apr. 2011.
- [4] T. G. Moore, "A FFT based algorithm for the formation of wide-angle ISAR images using EIP," in *Proc. IEEE International Radar Conference*, Alexandria, May 1995, pp.392-395.
- [5] I. Stojanovic, M. Cetin, and W. C. Karl, "Joint space aspect reconstruction of wide-angle SAR exploiting sparsity," in *SPIE Proc. Defense and Security Symposium*, Orlando, 2008, no.697005.
- [6] D. D. Lee, and H. S. Seung, "Learning the parts of objects by non-negative matrix factorization," *Nature*, vol.401, no.21, pp.788-791, Oct. 1999.
- [7] P. O. Hoyer, "Non-negative matrix factorization with sparseness constraints," *J. Mach. Learn. Res.*, vol. 5, pp. 1457–1469, Dec. 2004.
- [8] R. Guo, L. Zhang, M. Xing, and J. Li, "Polarimetric SAR image fusion using nonnegative matrix factorisation and improved-RGB model," *Electron.Lett.*, vol.46, no.20, pp.1399-1401, Sep. 2010.
- [9] N. Yokoya, T. Yairi, and A. Iwasaki, "Coupled nonnegative matrix factorization unmixing for hyperspectral and multispectral data fusion," *IEEE Trans. Geosci. Remote Sens.*, vol. 50, no. 2, pp. 528-537, Feb. 2012.
- [10] S. Jia and Y. Qian, "Constrained nonnegative matrix factorization for hyperspectral unmixing," *IEEE Trans. Geosci. Remote Sens.*, vol.50, no.2, pp. 161-173, Feb. 2012.
- [11] G. Fornaro, "Trajectory deviations in airborne SAR: analysis and compensation," *IEEE Trans. Aerosp. Electron. Syst.*, vol. 35, no. 3, pp. 997–1009, Jul. 1999.
- [12] H. Kim and H. Park, "Sparse non-negative matrix factorizations via alternating non-negativity-constrained least squares for micro array data analysis," *Bioinformatics*, vol. 23, no. 12, pp. 1495–1502, May 2007.
- [13] M. Cetin, "Feature-enhanced Synthetic Aperture Radar Imaging," Ph.D. dissertation, Boston Univ., Boston, MA, 2001.
- [14] D. D. Lee, and H. S. Seung, "Algorithms for non-negative matrix factorization," in *Proc. Neural Information Processing Systems Conference*, Vancouver, 2000, pp. 556-562.
- [15] O. Batu and M. Cetin, "Parameter selection in sparsity-driven SAR imaging," *IEEE Trans. Aerosp. Electron. Syst.*, vol. 47, no. 4, pp. 3040-3050, Oct. 2011.
- [16] Backhoe data dome and visual-D challenge problem. Air Force Research Laboratory Sensor Data Management System, 2004. [Online]. <https://www.sdms.afrl.af.mil/>.
- [17] M. Bucciarelli and D. Pastina, "Multi-grazing ISAR for side-view imaging with improved cross-range resolution," in *Proc. IEEE Radar Conference*, Kansas City, 2011, pp. 939-944.